

# A dynamical fossil in the Ursa Minor dwarf spheroidal galaxy

Jan T. Kleyrna<sup>1</sup>, Mark I. Wilkinson<sup>2</sup>, Gerard Gilmore<sup>3</sup>, N. Wyn Evans<sup>4</sup>,

<sup>1,2,3,4</sup>*Institute of Astronomy, Madingley Road, Cambridge, CB3 0HA, UK*

<sup>1</sup>*kleyrna@ast.cam.ac.uk*; <sup>2</sup>*markw@ast.cam.ac.uk*; <sup>3</sup>*gil@ast.cam.ac.uk*; <sup>4</sup>*nwe@ast.cam.ac.uk*

## ABSTRACT

The nearby Ursa Minor dwarf spheroidal (UMi dSph) is one of the most dark matter dominated galaxies known, with a central mass to light ratio  $M/L \sim 70$ . Somewhat anomalously, it appears to contain morphological substructure in the form of a second peak in the stellar number density. It is often argued that this substructure must be transient because it could not survive for the  $> 10$  Gyr age of the system, given the crossing time implied by UMi's  $8.8 \text{ km s}^{-1}$  internal velocity dispersion. In this paper, however, we present evidence that the substructure has a cold kinematical signature, and argue that UMi's clumpiness could indeed be a primordial artefact. Using numerical simulations, we demonstrate that substructure is incompatible with the cusped dark matter haloes predicted by the prevailing Cold Dark Matter (CDM) paradigm, but is consistent with an unbound stellar cluster sloshing back and forth within the nearly harmonic potential of a cored dark matter halo. Thus CDM appears to disagree with observation at the least massive, most dark matter dominated end of the galaxy mass spectrum.

*Subject headings:* galaxies: individual: Ursa Minor dSph – UMi – galaxies: kinematics and dynamics – Local Group – dark matter – celestial mechanics, stellar dynamics

## 1. Introduction

The CDM model of structure formation (e.g. Ostriker 1993) postulates that galaxies form when initial perturbations in a sea of cold (non-relativistic) dark matter particles seed the growth of larger dark matter haloes characterised by a central density cusp  $\rho(r) \propto r^{-a}$ , where  $a = 1$  to  $1.5$  (Navarro, Frenk, & White 1997; Ghigna et al. 2000). However, the rotation curves of massive galaxies almost invariably suggest that haloes have a flat density core rather than a sharp cusp (e.g. de Blok, McGaugh, & Rubin 2001). It has been suggested that an initial cusp may be destroyed by feedback mechanisms that couple supernovae driven

winds to the dark matter (e.g. Binney, Gerhard, & Silk 2001), but models of this sort have had mixed success.

The dSph galaxies (e.g. Mateo 1998) surrounding the Milky Way provide a good laboratory in which to test CDM predictions on small scales: most are sufficiently nearby to allow us to measure the velocities of hundreds of member stars, and most have such meagre baryonic content that their internal dynamics is everywhere dominated by the dark matter. Although it has argued for some time that CDM greatly overpredicts the number of dwarfs, some recent work (Stoehr et al. 2002) suggests that CDM is actually in good agreement with the local dSph population. Ursa Minor is, with Draco, one of the two most dark matter dominated dSphs of the Local Group, with a central mass to light ratio  $M/L \sim 70M_{\odot}/L_{\odot}$  (Hargreaves et al. 1994; Armandroff, Olszewski, & Pryor 1995). UMi’s stars appear to have been formed in a single burst (Carrera et al. 2002), and its size, stellar velocity dispersion, and luminosity resemble those of Draco, which has been shown to have a *mean* mass to light ratio  $M/L \sim 400M_{\odot}/L_{\odot}$  within three core radii (Kleyna et al. 2001). Unlike most other dSphs, however, UMi has substantial morphological distortions: UMi is highly elongated, and appears to possess a secondary clump or shoulder on the northeast side of the major axis (Irwin & Hatidimitriou 1995; Kleyna et al. 1998; Palma et al. 2002). It is often argued that this clump cannot be a persistent feature because the  $\sim 2 \times 10^7$  year stellar crossing time of the system is orders of magnitude shorter than its  $\sim 10^{10}$  year age, so that stellar orbits within an unbound clump will diverge over hundreds of dSph crossings. UMi’s relatively circular orbit (Schweitzer et al. 2003) weighs against the common explanation that the clump is a temporary artefact generated through ongoing tidal disruption by the Galaxy. Generally, models that attempt to explain the dSphs’ large velocity dispersions by tidal disruption still require dark matter, or else must postulate an unseen supply of dSphs to replace those that are disrupted (Oh, Lin, & Aarseth 1995), or require that dSphs are disintegrated remnants viewed along a very fortuitous line of sight (Kroupa 1997).

In this paper, we use a data set consisting of new and extant UMi stellar velocities to argue that the second peak in UMi’s stellar distribution has a cold kinematical signature, and we demonstrate that a plausible explanation is that the clump is a disrupted stellar cluster sloshing back and forth within UMi’s halo. We use numerical simulations and analytical arguments to show that persistent substructure is consistent with a cored halo, but not with a cusped CDM halo.

## 2. OBSERVATIONS AND ANALYSIS

In May 2002, we obtained spectra of 63 stars in UMi using the WYFFOS multifibre spectrograph at the William Herschel Telescope on La Palma. We cross-correlated the spectra with a synthetic template of the Ca triplet lines at  $\sim 850$  nm to measure velocities (e.g. Kleya et al. 2002); the median velocity error was  $5 \text{ km s}^{-1}$ , less than the UMi’s  $8.8 \text{ km s}^{-1}$  central velocity dispersion. As our stars were mostly at large projected radii in UMi, we combined our data with the more centrally concentrated sample of Armandroff et al. (1995), after subtracting the mean velocity difference of the two data sets. The combined data set contains 134 stars. Because the observing run was curtailed by bad weather, the data did not extend to a sufficiently large radius to allow a fit to the halo shape and anisotropy (c.f. Wilkinson et al. 2002; Kleya et al. 2002). However, we noted that a histogram of stellar velocities near the clump on the northeast side of UMi’s major axis appeared narrower than the  $8.8 \text{ km s}^{-1}$  Gaussian describing UMi’s overall line of sight velocity distribution (Figure 1). This observation suggested constructing a model of UMi’s population consisting of the sum of two Gaussians, one representing the underlying  $\sigma_0 = 8.8 \text{ km s}^{-1}$  Gaussian, and the other representing a sub-population of unknown fraction  $f$ , velocity offset  $v_s$ , and velocity dispersion  $\sigma_s$ . Assuming an observational velocity uncertainty  $\sigma_{\text{obs}}$ , the probability of observing a particular velocity in this model is

$$P(v|f, \sigma_s, \sigma_0, \sigma_{\text{obs}}) = f \times \frac{\exp\left[-\frac{1}{2} \frac{(v-v_s)^2}{\sigma_s^2 + \sigma_{\text{obs}}^2}\right]}{\sqrt{2\pi(\sigma_s^2 + \sigma_{\text{obs}}^2)}} + \quad (1)$$

$$(1 - f) \times \frac{\exp\left[-\frac{1}{2} \frac{v^2}{\sigma_0^2 + \sigma_{\text{obs}}^2}\right]}{\sqrt{2\pi(\sigma_0^2 + \sigma_{\text{obs}}^2)}}$$

and the likelihood of obtaining an ensemble of velocities  $\{v_i\}$  with errors  $\{\sigma_{\text{obs}i}\}$  is

$$P(\{v_i, \sigma_{\text{obs}i}\}) = \prod_i P(v_i|f, \sigma_s, \sigma_0, \sigma_{\text{obs}i}) \quad (2)$$

Next we scanned the face of UMi in RA and Dec in  $2'$  increments. At each point, we collected all velocities in a  $6'$  radius aperture, and computed the statistical likelihood of drawing these velocities from an  $8.8 \text{ km s}^{-1}$  Gaussian (Equation 2 with  $f = 0$ ), as well as the likelihood of drawing the velocities from each member of a grid of two-Gaussian models (Equation 2, with  $f = 0.1, 0.2 \dots 1.0$ ,  $v_s = -10, -9 \dots 10$ ,  $\sigma_s = 0.5, 1.0 \dots 15.0$ ). When the likelihood of the best-fitting two-Gaussian model exceeded the likelihood of the single Gaussian model by a large factor, we deemed that aperture to contain a kinematic subpopulation distinct from the rest of UMi’s stars. Figure 2 shows the result of the scanning procedure. Large dots

are apertures where we found a significant (likelihood ratio  $> 10^3$ ) sub-population. At the largest dot, the best two-Gaussian population ( $\sigma_s = 0.5 \text{ km s}^{-1}$ ,  $v_s = -1 \text{ km s}^{-1}$ ,  $f = 0.7$ ) is  $4.7 \times 10^4$  times more likely than the default  $8.8 \text{ km s}^{-1}$  single-Gaussian model. Moreover, the largest dot is very close to where the isopleth contours indicate the presence of a secondary peak in the stars. The small value of  $v_s$  suggests that the sub-population is either on a radial orbit or a face-on circular orbit. We note that our best-fit  $\sigma_s$  is ill-determined because it is much smaller than the velocity measurement errors. Also, this small value of  $\sigma_s$  applies only to the surviving phase space region of the progenitor cluster - any faster stars may have joined UMi's general population. We verified the statistical significance of the second kinematical population with a Monte-Carlo test: we repeatedly generated artificial data drawn from an  $8.8 \text{ km s}^{-1}$  Gaussian at the same locations and with the same velocity uncertainties as our actual data, and subjected it to the scanning procedure described above. We found that only 11 of 2000 (0.055%) artificial data sets give as large a likelihood ratio as the actual data anywhere in UMi. Only one of these false positives suggested an orbit in the plane of the sky, and all of the others had  $v_s > 5$ .

### 3. IMPLICATIONS OF THE COLD SUB-POPULATION

To investigate the survival of a cold kinematical sub-population in a dSph, we integrated the motion of a group of unbound stars inside a plausible halo model. We assumed a halo density law  $\rho(r) \propto (a^2 + r^2)^{-1/2}$ , which has a core for  $a > 0$  and a  $r^{-1}$  cusp for  $a = 0$ . We dropped an unbound clump modelled as a three dimensional spatial Gaussian with a three dimensional Gaussian velocity dispersion into this halo, and followed its evolution with an adaptive stepsize Runge-Kutta code for 12 Gyr. Using the mass of Draco as a reference (Kleyna et al. 2001), we normalised the enclosed mass of the model to  $5 \times 10^7 M_\odot$  inside  $r = 1$ , where  $r = 1$  corresponds to 600 pc, approximately the maximum extent of the stellar distribution. In our dimensionless units, the clump orbits within  $r = 0.25$ , or 150 pc in physical units.

Figure 3 shows the results of the simulations. When a clump with an initial one dimensional dispersion  $\sigma_s = 0.5 \text{ km s}^{-1}$  and a one-sigma radius of 0.02 (12 pc) is dropped at an initial radius  $r_0 = 0.25$  into a halo with an  $a = 0.85$  core (top panel) on near-radial orbit with a tangential velocity equal to 0.07 times the circular speed at  $r_0$ , the resulting sub-structure is visible for many Gyr. Even at 12 Gyr, nearly the age of the Universe, the remnants of the clump are spatially concentrated and asymmetrical. When an identical clump is dropped into a  $a = 0$  cusped halo (bottom panel) the clump dissipates completely within 1 Gyr.

The total velocity  $v = (v_x^2 + v_y^2 + v_z^2)^{1/2}$  histograms of Figure 3 demonstrate that the stars

remain cold for much of the evolution of the cored model, whereas they quickly achieve a flat distribution in a cusp. However, the fact that the orbit is constructed to be approximately in the plane of the sky implies that the measured line-of-sight  $v_z$  distribution remains cold for both the core and cusp. The distinguishing observable feature of the cored model, therefore, is a *localized* population that is cold in the line-of-sight.

Further simulations demonstrate that this conclusion holds good both for more circular orbits and for triaxial haloes. Cusps shallower than  $r^{-1}$  only slightly increase the longevity of the clump: for example, a clump in a  $\rho(r) \propto r^{-0.5}$  cusp survives approximately twice as long as in a  $r^{-1}$  cusp. If the halo core is an order of magnitude larger than the clump’s orbit, a clump can survive almost unaltered for a Hubble time. If the core radius is equal to or smaller than the clump’s orbit, however, the clump is destroyed within one or two Gyr. We conclude that a clump can survive for a large fraction of a Hubble time only if it is embedded in a core at least two or three times the size of its orbit.

An additional concern is the possibility that Galactic tides may destroy substructure in a cored halo. To address this point, we added the effect of tides to our simulation. We modelled the Galaxy as an isothermal sphere of mass  $10^{12} M_\odot$  inside 50 kpc, somewhat more massive than the value of Wilkinson & Evans (1999); at a 60 kpc apogalacticon, the tidal force from this Galaxy model is 0.02 times as strong as the dwarf’s gravity at a unitless dSph radius  $r = 1$ . We then created a varying tidal force in the dwarf’s  $x, y$  plane by moving the isothermal Galaxy model around the dSph on 1.6 Gyr orbits with eccentricities between 0 and 0.5. In no instance did this weak tidal force significantly affect the survival of substructure either in a core or in a cusp. Indeed, we could safely make the tidal force an order of magnitude larger without causing the clump to disintegrate in the above  $a = 0.85$  core.

We emphasize that these simulations are not in any sense a fit to the UMi data. Rather, they demonstrate that substructure can easily persist for many Gyr in a plausible cored halo, but is quickly erased in a cusp. Several unconstrained parameters affect the survival of substructure in a core. In addition to increasing the core size, for example, one can decrease the dSph’s mass, slowing the internal time scale and decreasing the number of orbits over which a clump can dissipate. Similarly, one can increase the longevity of the clump by decreasing its initial size or velocity dispersion. We find that strong substructure continues to persist for 12 Gyr when we double or treble the size or dispersion of our model clump in Figure 3, although the final distribution is less compact than in our illustrative example.

We note that there is a simple explanation for the persistence of a clump in any cored halo: a generic feature of dark matter haloes with cores is that the potential is close to that of a harmonic oscillator. The one dimensional  $x$  motion of a particle with position  $x_1$  and

velocity  $v_1$  at time  $t = 0$  is  $X_1(t) = x_1 \cos(\omega_x t) + v_1 \omega_x^{-1} \sin(\omega_x t)$ . Then the  $x$  distance between two particles dropped into a harmonic potential at positions and  $x_1, x_2$  with velocities  $0, v_2$  is given for all time as

$$X_1(t) - X_2(t) = (x_1 - x_2) \cos(\omega_x t) + x_2 \left( \frac{v_2}{x_2 \omega_x} \right) \sin(\omega_x t) \quad (3)$$

The cosine term is bounded by the initial separation, and the sine term is bounded by the orbital amplitude times the ratio of the relative speed (dispersion) to the orbital speed, in the approximation that the dispersion is smaller than the orbital speed. Because the three dimensions of the harmonic oscillator are independent, this result does not depend on spherical symmetry and is valid for any triaxial harmonic potential. Hence, if the non-harmonic terms of the Taylor expansion of the potential are sufficiently small, an unbound stellar clump with a small but finite internal dispersion can persist over a long time, pulsating in size without disintegrating.

In view of the above discussion, the fact that the tidal force only weakly affects clump survival is not surprising. The lowest order term of the tidal force arises from a rotating quadratic effective potential. This quadratic potential changes adiabatically, because the dwarf’s orbit around the Galaxy is  $\sim 10^2$  times longer than the internal time scale. Thus particles on adjacent sinusoidal orbits remain on adjacent sinusoidal orbits as the potential evolves.

The low-dispersion substructure that we observe in UMi is consistent with a clump progenitor similar to star clusters seen elsewhere in the Local Group. By rescaling the number of stars in the best aperture by the best-fit subpopulation fraction  $f = 0.7$ , we estimate that the clump contains  $\sim 7\%$  of UMi’s population. If we assume that UMi has a normal stellar mass to light ratio  $2M_\odot/L_\odot$  and a total V-band luminosity  $L_v \approx 2 \times 10^5 L_\odot$ , the clump has a luminosity of  $1.5 \times 10^4 L_\odot$  and a mass  $M = 3 \times 10^4 M_\odot$ . These parameters are similar to the low mass globular clusters in the SMC and LMC. A cluster with the mass of our clump and a half-mass radius  $r_{1/2} = 10$  pc has a characteristic one-dimensional internal velocity  $\sqrt{1/3} \sqrt{G(M/2)/r_{1/2}} \approx 1.5 \text{ km s}^{-1}$ , cold compared to UMi’s overall population. Such low-mass clusters can become unbound immediately after formation when supernovae expel the gas content (Goodwin 1997), or possibly slowly though tidal interactions with the parent galaxy’s halo (Giersz & Heggie 1997).

#### 4. CONCLUSIONS

Ursa Minor is known to possess a second peak in its stellar distribution. We demonstrate that the stars in the vicinity of this peak comprise a kinematically distinct cold sub-population; the probability of obtaining a similarly strong false positive in the absence of a sub-population is 0.055%. We show that the properties of this clump are consistent with the remnants of a disrupted stellar cluster orbiting in the plane of the sky within the harmonic potential of cored dark matter halo. Although a clump can persist for a Hubble time in a harmonic potential, the potential of a CDM cusped halo would destroy the clump within  $< 1$  Gyr. This finding suggests that the haloes of even the least massive, most dark matter dominated galaxies possess a core rather than a cusp.

NWE is supported by the Royal Society, while MIW and JK acknowledge support from PPARC. The authors gratefully thank the staff of the Isaac Newton Group for help in acquiring the data, and the anonymous referee for useful criticisms and suggestions.

#### REFERENCES

- Armandroff, T.E., Olszewski, E.W., & Pryor, C., 1995, *AJ*, 110, 2131
- Binney, J., Gerhard, O., & Silk, J., 2001, *MNRAS*, 321, 471
- de Blok, W.J.G., McGaugh, S.S., & Rubin, V.C., 2001, *AJ*, 122, 2396
- Carrera, R., Aparicio, A., Martínez-Delgado, D., & Alonso-García, J., 2002, *AJ*, 123, 3199
- Ghigna, S., Moore, B., Governato, F., Lake, G., Quinn, T. & Stadel, J., 2000, *ApJ*, 544, 616
- Giersz, M., & Heggie, D.C., 1997, *MNRAS*, 286, 709
- Goodwin, S.P., 1997, *MNRAS*, 286, 669
- Hargreaves, J.C., Gilmore, G., Irwin, M.J., Carter, D., 1994, *MNRAS*, 271, 693
- Irwin, M., Hatzidimitriou, D., 1995, *MNRAS*, 277, 1354
- Kleyna, J.T., Geller, M.J., Kurtz, M.J. & Thorstensen, J.R., 1998, *AJ*, 115, 2359
- Kleyna, J.T., Wilkinson, M.I., Evans, N.W., Gilmore G., 2001, *ApJ*, 563, L115
- Kleyna, J.T., Wilkinson M.I., Evans, N.W., Gilmore G., 2001, *MNRAS*, 330, 792

Kroupa, P., 1997, *New Astronomy*, 2, 139

Mateo, M., 1998, *ARA&A* 36, 435

Navarro, J.F.; Frenk, C.S.; White, S.D.M., 1997, *ApJ*, 490, 493

Oh, K.S., Lin, D.N.C. & Aarseth, S.J., 1995, *ApJ*, 442, 142

Ostriker, J., 1993, *ARA&A*, 6, 39

Palma, C., Majewski, S.R., Siegel, M.H., Patterson, R.J., Ostheimer, C., 2002, *astro-ph/0205194*

Schweitzer, A.E., Cudworth, K. M., & Majewski, S. R., 2003, *AJ*, submitted

Stoehr, F., White, S.D., Tormen, G., & Springel, V., 2002, *MNRAS* 335, L84

Wilkinson M.I., Kley, J.T., Evans, N.W., Gilmore G., 2001, *MNRAS*, 330, 778

Wilkinson M.I., Evans N.W., 1999, *MNRAS*, 310, 645



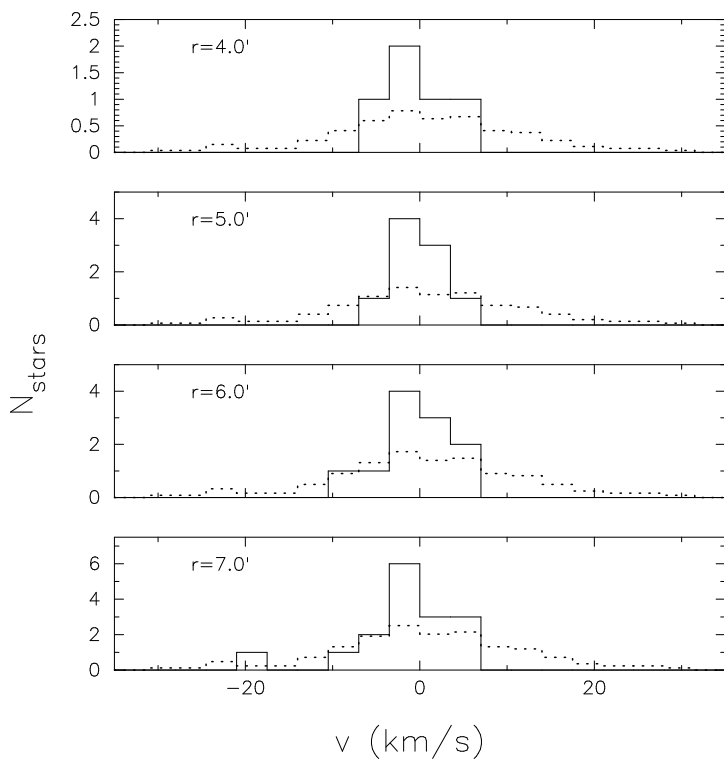


Fig. 1.— Solid histogram is UMi’s stellar velocity distribution inside apertures with diameters 4’ to 7’, centered on the location of second clump (RA = 12’, Dec = 8’ relative to UMi’s center; see Fig. 2). The dotted histogram is the distribution of velocities of the entire UMi sample, normalized to have the same number of stars as the solid histogram.

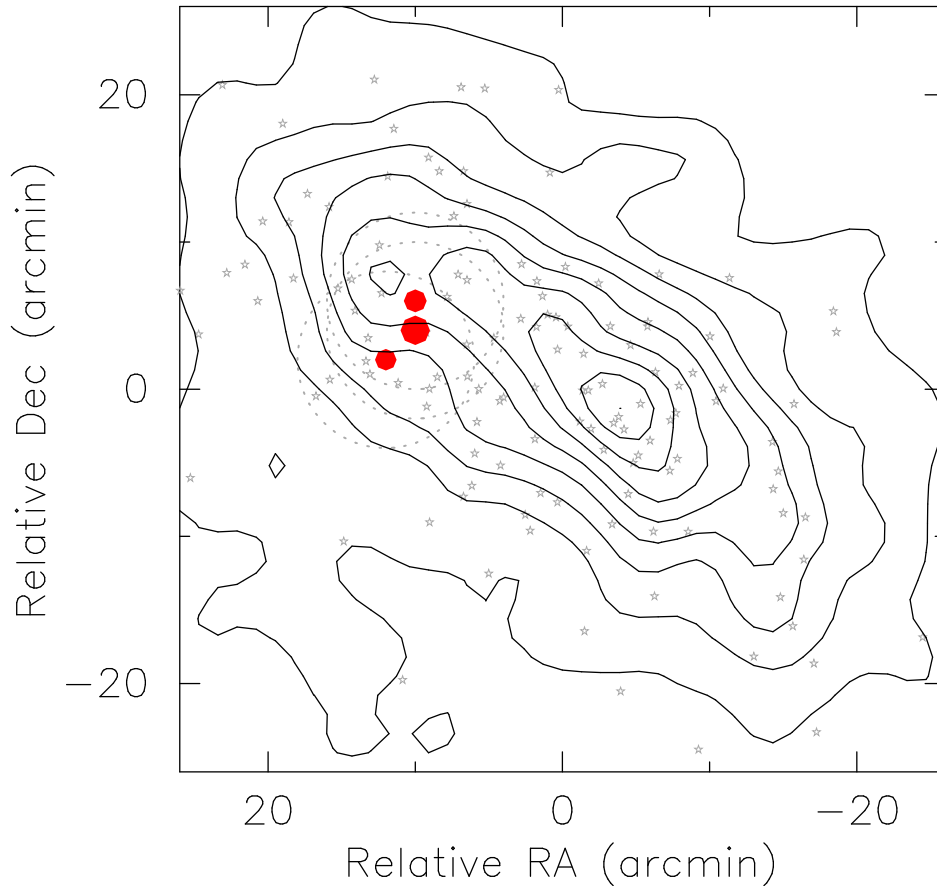


Fig. 2.— Result of search for kinematic sub-populations in UMi. Coutours are linearly spaced stellar isopleths; the second peak of UMi’s stellar population is visible at  $RA = 12'$ ,  $Dec = 8'$  relative to UMi’s center at  $15^{\text{h}}09^{\text{m}}10^{\text{s}}.2$ ,  $+67^{\circ}12'52''$  J2000. Gray stars are UMi RGB member stars with measured velocities. The filled circles represent points where a model with a kinematically cold sub-population is at least 1000 times more likely than a model composed of a single  $8.8 \text{ km s}^{-1}$  Gaussian. The dotted circles are the apertures containing the stellar sample for each dot. The size of each dot is proportional to the logarithm of the likelihood, and the largest dot represents a likelihood ratio of  $4.7 \times 10^4$ , with an optimal clump fraction  $f = 0.7$ , mean clump velocity  $v_s = -1 \text{ km s}^{-1}$ , and clump dispersion  $\sigma_s = 0.5 \text{ km s}^{-1}$ .

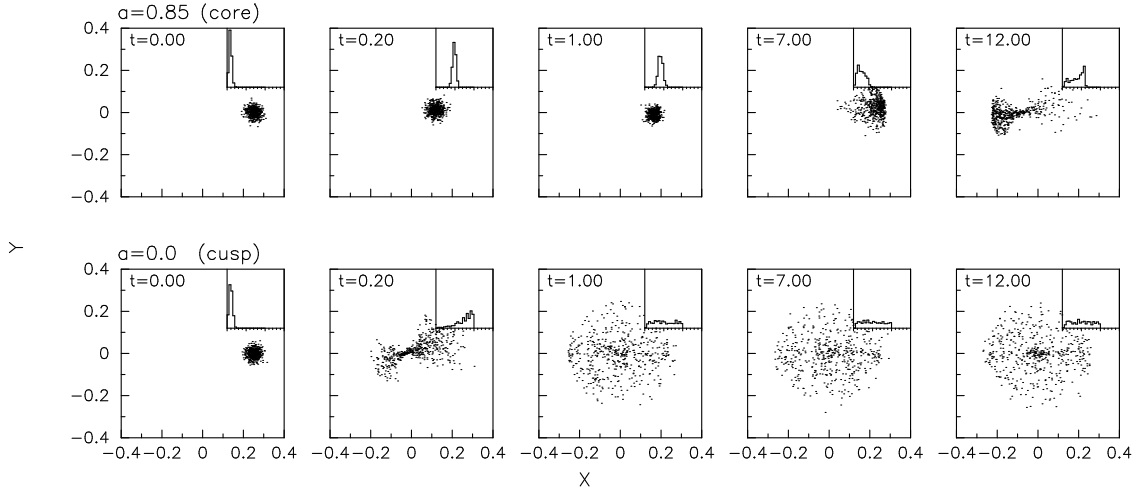


Fig. 3.— Simulation of an unbound clump in a dark matter halo. The halo has a density law  $\rho(r) \propto (a^2 + r^2)^{-1/2}$  and a mass of  $5 \times 10^7 M_\odot$  inside  $r = 1$ , which corresponds to 600 pc. The clump has an initial one-dimensional dispersion of  $0.5 \text{ km s}^{-1}$  and an initial speed equal to 0.05 times the circular speed in each of the  $y$  and  $z$  directions; the time  $t$  is in units of Gyr. Top panel: a clump in a cored halo with  $a = 0.85$  persists for a Hubble time because the potential is nearly harmonic. Bottom panel: a clump in a cusped potential ( $a = 0$ ) disrupts in less than 1 Gyr. The histograms at the upper right corner of each snapshot show the distribution of total velocity  $v = (v_x^2 + v_y^2 + v_z^2)^{1/2}$ ; tick marks are spaced  $1 \text{ km s}^{-2}$  apart. As is expected, the stars in a cored halo remain coherent in velocity as well as in position.